

World Journal of *Gastroenterology*

World J Gastroenterol 2021 November 21; 27(43): 7402-7581



FRONTIER

- 7402 Antimicrobial peptides and the gut microbiome in inflammatory bowel disease
Gubatan J, Holman DR, Puntasecca CJ, Polevoi D, Rubin SJ, Rogalla S
- 7423 Idiopathic chronic pancreatitis: Beyond antioxidants
Mehta RM, Pandol SJ, Joshi PR

OPINION REVIEW

- 7433 COVID-19 as a trigger of irritable bowel syndrome: A review of potential mechanisms
Settanni CR, Ianiro G, Ponziani FR, Bibbò S, Segal JP, Cammarota G, Gasbarrini A

REVIEW

- 7446 Overview of the microbiota in the gut-liver axis in viral B and C hepatitis
Neag MA, Mitre AO, Catinean A, Buzoianu AD
- 7462 Hepatocellular carcinoma locoregional therapies: Outcomes and future horizons
Makary MS, Ramsell S, Miller E, Beal EW, Dowell JD

MINIREVIEWS

- 7480 Recent advances in artificial intelligence for pancreatic ductal adenocarcinoma
Hayashi H, Uemura N, Matsumura K, Zhao L, Sato H, Shiraishi Y, Yamashita YI, Baba H
- 7497 Hepatitis B: Who should be treated?-managing patients with chronic hepatitis B during the immune-tolerant and immunoactive phases
Kawanaka M, Nishino K, Kawamoto H, Haruma K

ORIGINAL ARTICLE**Basic Study**

- 7509 Liver injury changes the biological characters of serum small extracellular vesicles and reprograms hepatic macrophages in mice
Lv XF, Zhang AQ, Liu WQ, Zhao M, Li J, He L, Cheng L, Sun YF, Qin G, Lu P, Ji YH, Ji JL
- 7530 Genome-wide map of N⁶-methyladenosine circular RNAs identified in mice model of severe acute pancreatitis
Wu J, Yuan XH, Jiang W, Lu YC, Huang QL, Yang Y, Qie HJ, Liu JT, Sun HY, Tang LJ
- 7546 Survivin-positive circulating tumor cells as a marker for metastasis of hepatocellular carcinoma
Yu J, Wang Z, Zhang H, Wang Y, Li DQ

Prospective Study

- 7563** Immunoglobulin G in non-alcoholic steatohepatitis predicts clinical outcome: A prospective multi-centre cohort study

De Roza MA, Lamba M, Goh GBB, Lum JHM, Cheah MCC, Ngu JHJ

SYSTEMATIC REVIEWS

- 7572** Minimum sample size estimates for trials in inflammatory bowel disease: A systematic review of a support resource

Gordon M, Lakunina S, Sinopoulou V, Akobeng A

ABOUT COVER

Editorial Board Member of *World Journal of Gastroenterology*, Serag M Esmat, MD, Professor, Department of Internal Medicine, Faculty of Medicine, Cairo University, Cairo 11562, Egypt. seragesmat@kasralainy.edu.eg

AIMS AND SCOPE

The primary aim of *World Journal of Gastroenterology* (WJG, *World J Gastroenterol*) is to provide scholars and readers from various fields of gastroenterology and hepatology with a platform to publish high-quality basic and clinical research articles and communicate their research findings online. WJG mainly publishes articles reporting research results and findings obtained in the field of gastroenterology and hepatology and covering a wide range of topics including gastroenterology, hepatology, gastrointestinal endoscopy, gastrointestinal surgery, gastrointestinal oncology, and pediatric gastroenterology.

INDEXING/ABSTRACTING

The WJG is now indexed in Current Contents®/Clinical Medicine, Science Citation Index Expanded (also known as SciSearch®), Journal Citation Reports®, Index Medicus, MEDLINE, PubMed, PubMed Central, and Scopus. The 2021 edition of Journal Citation Report® cites the 2020 impact factor (IF) for WJG as 5.742; Journal Citation Indicator: 0.79; IF without journal self cites: 5.590; 5-year IF: 5.044; Ranking: 28 among 92 journals in gastroenterology and hepatology; and Quartile category: Q2. The WJG's CiteScore for 2020 is 6.9 and Scopus CiteScore rank 2020: Gastroenterology is 19/136.

RESPONSIBLE EDITORS FOR THIS ISSUE

Production Editor: Yan-Xia Xing; Production Department Director: Xiang Li; Editorial Office Director: Ze-Mao Gong.

NAME OF JOURNAL

World Journal of Gastroenterology

ISSN

ISSN 1007-9327 (print) ISSN 2219-2840 (online)

LAUNCH DATE

October 1, 1995

FREQUENCY

Weekly

EDITORS-IN-CHIEF

Andrzej S Tarnawski, Subrata Ghosh

EDITORIAL BOARD MEMBERS

<http://www.wjgnet.com/1007-9327/editorialboard.htm>

PUBLICATION DATE

November 21, 2021

COPYRIGHT

© 2021 Baishideng Publishing Group Inc

INSTRUCTIONS TO AUTHORS

<https://www.wjgnet.com/bpg/gerinfo/204>

GUIDELINES FOR ETHICS DOCUMENTS

<https://www.wjgnet.com/bpg/GerInfo/287>

GUIDELINES FOR NON-NATIVE SPEAKERS OF ENGLISH

<https://www.wjgnet.com/bpg/gerinfo/240>

PUBLICATION ETHICS

<https://www.wjgnet.com/bpg/GerInfo/288>

PUBLICATION MISCONDUCT

<https://www.wjgnet.com/bpg/gerinfo/208>

ARTICLE PROCESSING CHARGE

<https://www.wjgnet.com/bpg/gerinfo/242>

STEPS FOR SUBMITTING MANUSCRIPTS

<https://www.wjgnet.com/bpg/GerInfo/239>

ONLINE SUBMISSION

<https://www.f6publishing.com>

Basic Study

Genome-wide map of N⁶-methyladenosine circular RNAs identified in mice model of severe acute pancreatitis

Jun Wu, Xiao-Hui Yuan, Wen Jiang, Yi-Chen Lu, Qi-Lin Huang, Yi Yang, Hua-Ji Qie, Jiang-Tao Liu, Hong-Yu Sun, Li-Jun Tang

ORCID number: Jun Wu 0000-0003-1555-8026; Xiao-Hui Yuan 0000-0002-6462-2672; Wen Jiang 0000-0001-6823-6122; Yi-Chen Lu 0000-0002-4020-4847; Qi-Lin Huang 0000-0002-0819-4829; Yi Yang 0000-0002-0189-6246; Hua-Ji Qie 0000-0002-6648-7339; Jiang-Tao Liu 0000-0002-5993-8103; Hong-Yu Sun 0000-0002-8587-0499; Li-Jun Tang 0000-0001-6000-9515.

Author contributions: Wu J and Yuan XH contributed equally to this work; Tang LJ and Sun HY participated in the study conception and design; Wu J and Yuan XH participated in the writing of the main manuscript; Wu J, Yuan XH, Jiang W and Lu YC participated in the performance of the experiments; Huang QL and Yang Y participated in statistical data analysis and interpretation; Qie HJ and Liu JT participated in the preparation of figures; Tang LJ and Sun HY participated in the revision of the manuscript and final approval.

Institutional review board

statement: The study was reviewed and approved by the Institutional Ethics Committee at the General Hospital of Western Theater Command (Chengdu, China), No. A20190252005.

Jun Wu, Xiao-Hui Yuan, Wen Jiang, Yi-Chen Lu, Qi-Lin Huang, Yi Yang, Hua-Ji Qie, Jiang-Tao Liu, Hong-Yu Sun, Li-Jun Tang, Department of General Surgery and Pancreatic Injury and Repair Key Laboratory of Sichuan Province, The General Hospital of Western Theater Command, Chengdu 610036, Sichuan Province, China

Jun Wu, Xiao-Hui Yuan, Wen Jiang, Yi-Chen Lu, Hua-Ji Qie, Jiang-Tao Liu, Hong-Yu Sun, Li-Jun Tang, College of Medicine, Southwest Jiaotong University, Chengdu 610036, Sichuan Province, China

Hong-Yu Sun, Laboratory of Basic Medicine, The General Hospital of Western Theater Command, Chengdu 610036, Sichuan Province, China

Corresponding author: Li-Jun Tang, MD, PhD, Chief Doctor, Professor, Department of General Surgery and Pancreatic Injury and Repair Key Laboratory of Sichuan Province, The General Hospital of Western Theater Command, No. 270 Tianhuan Road, Furong Avenue, Jinniu District, Chengdu 610036, Sichuan Province, China. tanglj2016@163.com

Abstract**BACKGROUND**

Severe acute pancreatitis (SAP) is a deadly inflammatory disease with complex pathogenesis and lack of effective therapeutic options. N⁶-methyladenosine (m⁶A) modification of circRNAs plays important roles in physiological and pathological processes. However, the roles of m⁶A circRNA in the pathological process of SAP remains unknown.

AIM

To identify transcriptome-wide map of m⁶A circRNAs and to determine their biological significance and potential mechanisms in SAP.

METHODS

The SAP in C57BL/6 mice was induced using 4% sodium taurocholate salt. The transcriptome-wide map of m⁶A circRNAs was identified by m⁶A-modified RNA immunoprecipitation sequencing. The biological significance of circRNAs with differentially expressed m⁶A peaks was evaluated through gene ontology and Kyoto Encyclopedia of Genes and Genomes analysis. The underlying mechanism of m⁶A circRNAs in SAP was analyzed by constructing of m⁶A circRNA-microRNA networks. The expression of demethylases was determined by

Institutional animal care and use committee statement: The experimental procedures were reviewed and approved by the Institutional Animal Care and Use Committee at the General Hospital of Western Theater Command (Chengdu, China), and were conducted in accordance with the established International Guiding Principles for Animal Research.

Conflict-of-interest statement: The authors declare that there is no conflict of interest related to this study.

Data sharing statement: We had submitted the data to the online repository, which can be found at: <https://www.ncbi.nlm.nih.gov/gco/query/acc.cgi?acc=GSE173298>.

ARRIVE guidelines statement: The authors have read the ARRIVE guidelines, and the manuscript was prepared and revised according to the ARRIVE guidelines.

Supported by the National Natural Science Foundation of China, No. 81772001; and the National Clinical Key Subject of China, No. 41732113.

Country/Territory of origin: China

Specialty type: Gastroenterology and hepatology

Provenance and peer review: Unsolicited article; Externally peer reviewed.

Peer-review report's scientific quality classification

Grade A (Excellent): 0
Grade B (Very good): B, B
Grade C (Good): 0
Grade D (Fair): D
Grade E (Poor): 0

Open-Access: This article is an open-access article that was selected by an in-house editor and fully peer-reviewed by external reviewers. It is distributed in accordance with the Creative Commons Attribution NonCommercial (CC BY-NC 4.0) license, which permits others to distribute, remix, adapt, build

quantitative polymerase chain reaction and western blot to deduce the possible mechanism of reversible m⁶A process in SAP.

RESULTS

Fifty-seven circRNAs with differentially expressed m⁶A peaks were identified by m⁶A-modified RNA immunoprecipitation sequencing, of which 32 were upregulated and 25 downregulated. Functional analysis of these m⁶A circRNAs in SAP found some important pathways involved in the pathogenesis of SAP, such as regulation of autophagy and protein digestion. In m⁶A circRNA-miRNA networks, several important miRNAs participated in the occurrence and progression of SAP were found to bind to these m⁶A circRNAs, such as miR-24-3p, miR-26a, miR-92b, miR-216b, miR-324-5p and miR-762. Notably, the total m⁶A level of circRNAs was reduced, while the demethylase alkylation repair homolog 5 was upregulated in SAP.

CONCLUSION

m⁶A modification of circRNAs may be involved in the pathogenesis of SAP. Our findings may provide novel insights to explore the possible pathogenetic mechanism of SAP and seek new potential therapeutic targets for SAP.

Key Words: Severe acute pancreatitis; Circular RNAs; N⁶-methyladenosine; MeRIP-seq; Epigenetic analysis

©The Author(s) 2021. Published by Baishideng Publishing Group Inc. All rights reserved.

Core Tip: We identified a transcriptome-wide map of N⁶-methyladenosine (m⁶A) circRNAs and determined their biological significance and potential mechanisms in severe acute pancreatitis (SAP). The main findings were: (1) Function analysis found that circRNAs with differentially expressed m⁶A peaks were involved in the key process of SAP; (2) m⁶A may affect the interplays of circRNAs and microRNAs to participate in the pathogenesis of SAP; and (3) Demethylase alkylation repair homolog 5 may play key roles in dynamic process of m⁶A to downregulate the total m⁶A level of circRNAs in SAP. We provided novel insights to explore the possible pathophysiological mechanism of SAP and seek new potential therapeutic targets.

Citation: Wu J, Yuan XH, Jiang W, Lu YC, Huang QL, Yang Y, Qie HJ, Liu JT, Sun HY, Tang LJ. Genome-wide map of N⁶-methyladenosine circular RNAs identified in mice model of severe acute pancreatitis. *World J Gastroenterol* 2021; 27(43): 7530-7545

URL: <https://www.wjgnet.com/1007-9327/full/v27/i43/7530.htm>

DOI: <https://dx.doi.org/10.3748/wjg.v27.i43.7530>

INTRODUCTION

Acute pancreatitis (AP) is a pancreatic inflammatory disorder that is associated with substantial morbidity and mortality[1]. Approximately 20% of patients with AP develop into severe AP (SAP)[2]. Due to the extensive pancreatic necrosis, subsequent infection, systemic inflammatory response syndrome and multiple organ failure, the mortality of SAP is up to 30%[2,3]. Previous studies have suggested that some important pathological mechanisms, including premature trypsinogen activation in the acinar cells and macrophages, mitochondrial dysfunction, pathological calcium signaling, endoplasmic reticulum (ER) stress, and impaired autophagy, are involved in the initiation and development of SAP[1]. However, the pathophysiology of SAP is complex and remains unclear, especially the level of gene regulation.

CircRNAs were discovered in the 1970s[4] and were identified as single-stranded covalently closed RNA molecules that lack 5' caps and 3' tails[5]. Long after, they were thought to be the byproducts of splicing[6]. In recent years, as high-throughput sequencing developed, thousands of circRNAs were found to be expressed in a wide range of mammalian tissues[7,8], including the pancreas[9], and accumulating studies have demonstrated that circRNAs play vital roles in the whole process and prognosis

upon this work non-commercially, and license their derivative works on different terms, provided the original work is properly cited and the use is non-commercial. See: <http://creativecommons.org/licenses/by-nc/4.0/>

Received: May 19, 2021

Peer-review started: May 19, 2021

First decision: June 22, 2021

Revised: June 23, 2021

Accepted: September 15, 2021

Article in press: September 15, 2021

Published online: November 21, 2021

P-Reviewer: Kontos CK, Surbatovic M

S-Editor: Wu YXJ

L-Editor: Filipodia

P-Editor: Xing YX



of many diseases, including cardiovascular diseases[8], cancer[10], neurodevelopmental processes[11], immune responses and immune diseases[12]. The main mechanisms of circRNAs participated in the initiation and development of diseases include the following functions[6,8,10,12]: interplay with RNA-binding proteins, microRNA (miRNA) sponges, regulating the stability of mRNAs, modulating the transcription of parental gene and the templates for protein synthesis. However, the post-transcription modification of circRNAs remains unclear.

N⁶-methyladenosine (m⁶A) is the most prevalent internal modification of RNA in eukaryotic cells[13]. In 2017, Zhou *et al*[14] reported that the m⁶A modification is widespread in circRNAs and m⁶A modifications are read and written by the same complexes in circRNAs and mRNAs. The regulatory role of m⁶A is mainly performed by three homologous factors, namely so-called “writers”, “erasers” and “readers”[13-15]. The writers mainly include methyltransferase-like 3 and 14 proteins (METTL3 and METTL14) and their cofactor WT1-associated protein (WTAP). They form a methyltransferase complex to catalyze the installation of m⁶A. The erasers, including alkylation repair homolog 5 (ALKBH5) and fat mass and obesity related protein (FTO), can catalyze the oxidative demethylation of N-alkylated nucleic acid bases. The readers are mainly YT521-B homology (YTH) domain containing proteins family, including YTHDC1, YTHDC2, YTHDF1, YTHDF2 and YTHDF3. They can specifically recognize m⁶A and regulate splicing, localization, degradation and translation of RNAs. Recently, it has been found that the m⁶A modification of circRNAs plays a key role in innate immunity and tumors through regulating the metabolism and function of circRNAs[15]. In human embryonic stem cells and HeLa cells, m⁶A circRNAs display cell-type-specific methylation patterns[14]. In colorectal carcinoma, the m⁶A modification can modulate cytoplasmic export of circNSUN2 and stabilize HMGGA2, ultimately enhancing the colorectal liver metastasis[16]. However, the roles of m⁶A circRNAs in SAP are still unknown.

Here, we investigated the expression profile of m⁶A circRNAs in SAP through m⁶A-modified RNA immunoprecipitation sequencing (MeRIP-seq). We evaluated the biological significance of circRNAs with differentially expressed m⁶A peaks through gene ontology (GO) analysis, Kyoto Encyclopedia of Genes and Genomes (KEGG) pathway analysis, and explored their underlying mechanism by construction of m⁶A circRNA-miRNA networks. In addition, we determined the expression of demethyltransferase, ALKBH5 and FTO, to deduce the possible mechanism of reversible m⁶A process in SAP.

MATERIALS AND METHODS

Animals and preparation of SAP model

Male C57BL/6 mice weighing 22-25 g were provided by Chengdu Dashuo Experimental Animal Technology Co. Ltd. All the mice were housed in ventilated plastic cage system and fed with the same food and water for 7 d to adapt to the environment. The entire research protocol was approved by the Institutional Animal Care and Use Committee at the General Hospital of Western Theater Command.

Before the operation, the mice were divided into SAP and control groups randomly (3 mice per group) and fasted for 12 h but had free access to water. Isoflurane (5%) was used to anesthetize mice by induction box prior to surgery. Then, the SAP was induced through 4% sodium taurocholate salt that was slowly retrogradely injected into the biliopancreatic duct with a microinfusion pump. All mice were killed 24 h after the establishment of model, and the blood samples and pancreatic tissues were collected for further analysis.

Pancreatic histological analysis

Pancreatic tissue (0.4 cm × 0.4 cm) was fixed in 4% paraformaldehyde solution. After dehydrating with ethanol, the tissue samples were embedded in paraffin. Then, the samples were cut into about 4-μm-thick sections, and the sections were stained with hematoxylin and eosin. The light microscopy at × 200 magnification was used to examine the slide. The scoring system described previously was used to evaluate the degree of pancreatic injury[17]. The scores were averaged for five different slides that were selected randomly from each pancreas.

Amylase and lipase measurement

The concentrations of lipase and amylase in serum were determined using Lipase Assay kit and Amylase Assay kit (Nanjing Jiancheng Bioengineering Institute,

Nanjing, China) according to the instructions.

RNA isolation and RNA quality control

TRIzol reagent (Invitrogen, Carlsbad, CA, United States) was used to extract total RNA from the homogenized pancreatic tissues of the control and SAP groups. The concentration of extracted RNA was measured at OD₂₆₀ and 280 by NanoDrop ND-2000 instrument (Thermo Fisher Scientific, Waltham, MA, United States). We assessed the integrity of RNA through denaturing agarose gel electrophoresis. The OD A₂₆₀/A₂₈₀ ratio between 1.8 and 2.0 was set as the RNA purity standard.

Library preparation and MeRIP-seq

rRNAs in total RNA were removed using Ribo-Zero rRNA Removal Kits (Illumina, San Diego, CA, United States). The removal efficiency of rRNA by the residual determination of 28S and 18S of rRNA using quantitative polymerase chain reaction (qPCR). The fragmented RNA was incubated with the anti-m⁶A antibody at 4 °C for 2 h in IPP buffer. Then, the mixture was immunoprecipitated by incubation with protein-A beads (Thermo Fisher Scientific) for 2 h at 4 °C. The bound RNA was eluted from the beads with m⁶A (Berry & Associates) in IPP buffer and then extracted with TRIzol reagent (Thermo Fisher Scientific). The immunoprecipitated RNA and input RNA were used to construct the library using NEBNext[®] Ultra™ RNA Library Prep Kit and double-ended 150-bp sequencing of the m⁶A-IP and input samples was performed on an Illumina HiSeq sequencer (performed by Cloudseq Biotech Inc., Shanghai, China).

Analysis of MeRIP-Seq data

Paired-end reads were harvested from the Illumina HiSeq 4000 sequencer, and were quality controlled by Q30. To obtain high quality clean reads, 3' adaptor-trimming and low-quality reads were removed by cutadapt software. The clean reads with high quality of the input library were aligned to the mouse reference genome (UCSC MM10) with STAR software. DCC software was used for detecting and identifying the circRNAs. The identified circRNAs were annotated using the circBase database and Circ2Traits database. For all samples, raw junction reads were normalized to the number of total mapped reads and log₂ transformed. The read alignments on the genome were visualized using the tool integrative genomics viewer. The adapter-removal reads were aligned to the reference genome using Hisat2 software. The methylated sites in each sample were identified using MACS software. Differentially methylated sites were identified using diffReps software.

GO and KEGG analysis

The parent genes of circRNAs with differential m⁶A peaks were selected to analyze their potential biological roles through GO and KEGG pathway analysis. GO analysis included three parts, namely, biological process (BP) analysis, molecular function (MF) analysis, and cell component (CC) analysis[18]. GO analysis was performed by R topGO package. Fisher's exact test in Matlab MCR software was applied to calculate the enrichment of each pathway. The bubble plots and column plots were generated using the ggplot2 in R package (<https://ggplot2.tidyverse.org>).

Construction of circRNA-miRNA networks

circRNA containing miRNA-binding sites can bind to miRNA response elements competitively, further regulating the target mRNAs[19]. The top 10 upregulated and top 10 downregulated circRNAs according to the level of m⁶A were selected to construct circRNA-miRNA networks. The m⁶A circRNA-miRNA networks were constructed using TargetScan software and miRanda software and the circRNA-miRNA interactions were visualized by Cytoscape.

Conservation analysis

The top 10 upregulated and top 10 downregulated circRNAs were selected to analyze their homology with human circRNAs. The sequence of human circRNAs was downloaded from circBase database and the sequence of each selected m⁶A circRNA was blasted against the human circRNAs sequence by the blastn function of Blast software.

Western blotting

The whole pancreatic tissues from SAP and control groups were placed in RIPA lysate buffer with protease inhibitor, phosphatase inhibitor and phenylmethylsulfonyl fluoride inside (Total Protein Extraction Kit; Beijing Solarbio Science and Technology

Inc., Beijing, China), and the tissues were homogenized with homogenizer. The tissue homogenate was centrifuged at 12000 g for 30 min at 4 °C, and the supernatant was collected. After protein concentration was measured by BCA Protein Assay Kit (Beyotime Biotechnology, Jiangsu, China), the supernatant was mixed with loading buffer (Beijing Solarbio Science and Technology), boiled at 100 °C for 10 min for protein denaturation, and stored at -80 °C after separation. The target proteins were separated by SDS-PAGE. The proteins were transferred to polyvinylidene difluoride membrane (0.45 μm, IPVH00010; Millipore, Billerica, MA, United States), blocked in 5% nonfat milk for 1 h at room temperature (22 ± 3 °C), and then incubated with primary antibody, FTO (1:1000, D2V1I; Cell Signaling Technology, Danvers, MA, United States), ALKBH5 (1:2000, 16837-1-AP; Proteintech, Rosemont, IL, United States), GAPDH (1:5000, 10494-1-AP; Proteintech) at 4 °C overnight. The membranes were washed with Tris-buffered saline with Tween-20 (TBST) (Beijing Solarbio Science and Technology) three times and incubated with secondary antibody (1:10000, 15015; Proteintech) at room temperature for 1 h. After being washed three times with TBST, the protein bands were visualized by enhanced chemiluminescence (Immobilon Western Chemilum HRP Substrate; Millipore) in a biological imaging system.

qPCR

The total RNA was extracted from SAP and control groups as described above. qPCR was performed using One Step SYBR[®] PrimeScript[™] RT-PCR kit II (Takara Biotechnology Co., Ltd., Dalian, China) and the primers (ALKBH5: forward 5'-GGCGGTCAT-CATTCTCAGGAAGAC-3' and reverse 5'-CTGACAGGCGATCTGAAGCATAGC-3'; FTO: forward 5'-CTCACAGCC TCGGTTTAGTTCCAC-3' and reverse 5'-CGTCGC-CATCGTCTGAGTCATT G-3'; GAPDH: forward 5'-GGTGAAGGTCGGTGTGAACG-3' and reverse 5'-CTCGCTCCTGGAAGATGGTG-3') were synthesized by Shanghai Sangon Biotech Co., Ltd.. The outcomes were analyzed by means of 2^{-ΔΔCT} through normalizing the quantity of GAPDH.

Data analysis

GraphPad Prism 8 (La Jolla, CA, United States) and SPSS 22.0 (IBM Corp., Armonk, NY, United States) were used for performing statistical analyses. Student's *t* test was used for estimating statistically significance between two groups. The results were evaluated through Spearman's correlation coefficient test. All values are shown as mean ± SE of the mean; *P* < 0.05 was regarded as statistically significant.

RESULTS

Evaluation of mouse model of SAP

Twenty-four hours after treatment with sodium taurocholate salt, the staining of hematoxylin and eosin on the pancreatic tissues from the SAP group showed typical histopathological changes, including pancreatic lobular edema, extensive acinar cell necrosis, focal expansion of the pancreatic interlobular septum and granulocyte infiltration (Figure 1A). By contrast, under light microscopy, the pancreases from the control group had a complete normal structure. Figure 1B showed the corresponding histopathological scores. At the same time, considering that the levels of serum lipase and amylase are as one of the diagnostic criteria of AP[20], we determined their concentrations in serum. As a result, the serum lipase and amylase levels in the SAP group were also markedly higher than those in the control group (*P* < 0.05; Figure 1C and 1D). These results confirmed the successful establishment of the SAP mice model.

Overview of m⁶A circRNAs in SAP

We used MeRIP-seq to investigate the expression of m⁶A circRNAs in pancreatic tissues from the control and SAP groups. We had submitted the data to the online repository, which can be found at: <https://www.ncbi.nlm.nih.gov/geo/query/acc.cgi?acc=GSE173298>. Before performing MeRIP-seq, the residual determination of 28S and 18S of rRNA showed that the rRNAs in total RNA were removed effectively (Supplementary Figure 1). In general, a total of 409 m⁶A circRNAs were identified in all chromosomes (Figure 2A). Among these, 178 were specifically expressed in the SAP group, 107 in the control group, and 124 were shared in both groups (Figure 2B). m⁶A level in total circRNAs from the SAP group was lower than that from the control group (Figure 2C). Besides, > 80% of circRNAs contained only one m⁶A peak in both SAP and control groups (Figure 2D).

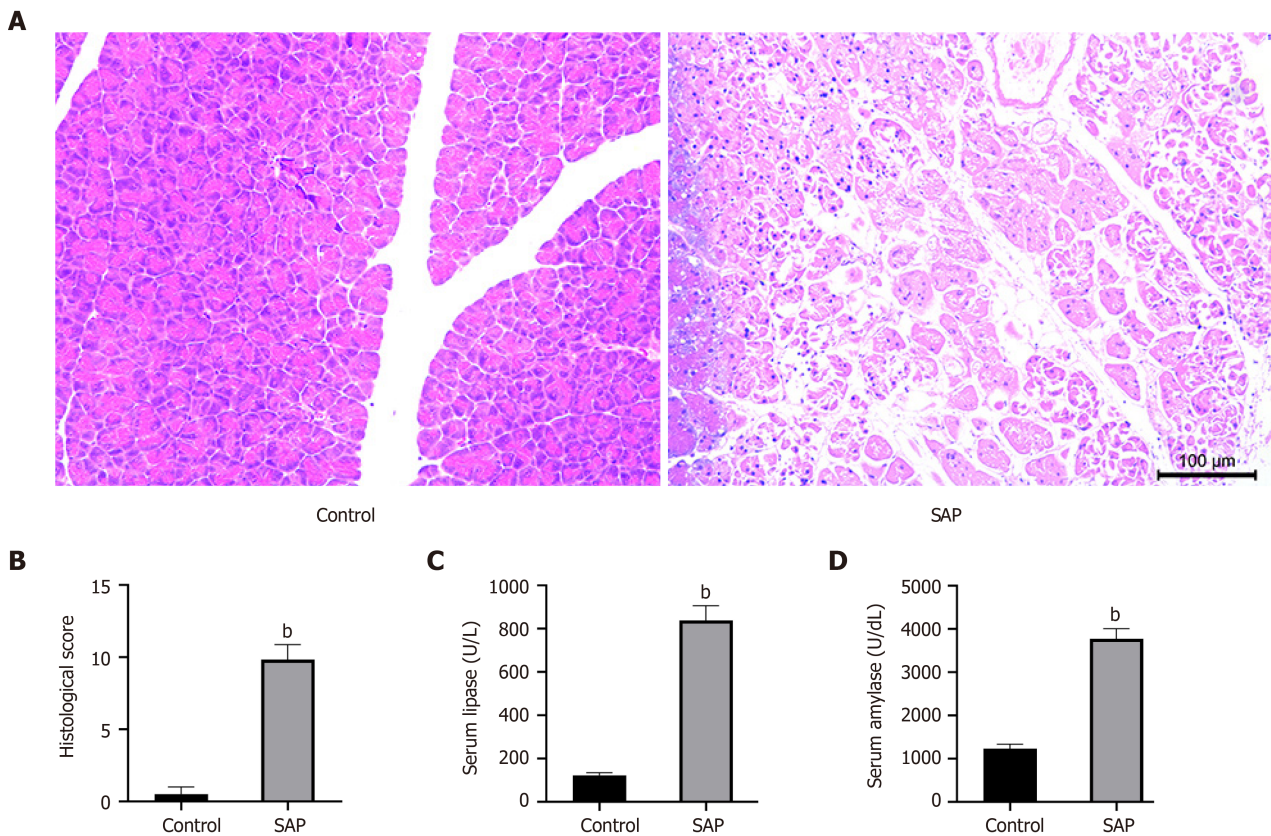


Figure 1 Evaluation of mouse model of severe acute pancreatitis. A: Representative images of pancreatic tissues stained with hematoxylin from control (left) and severe acute pancreatitis (SAP) (right) groups ($\times 100$ magnification); B: Histological score of pancreatic tissues in control and SAP groups; C and D: Levels of serum lipase and amylase, respectively. ^b $P < 0.01$ vs control group, $n = 3$ per group.

Differential m⁶A modification of circRNAs in SAP

To understand the biological role of m⁶A modification of circRNAs in SAP, the circRNAs with differentially expressed (DE) m⁶A peaks were further analyzed. Significant differential expression was defined as fold-change > 2 and $P < 0.05$. Compared with the control group, 57 circRNAs with DE m⁶A peaks were identified; 32 were upregulated and 25 downregulated in the SAP group. Table 1 presents the top 10 methylated m⁶A sites that were up- and downregulated within circRNAs. Figure 3A shows the m⁶A circRNAs expression profile in the SAP and control groups through hierarchical cluster analysis. The scatter plot exhibits the variation of DE m⁶A circRNAs between the SAP and control groups (Figure 3B). The volcano plot depicted DE m⁶A circRNAs between the two groups (Figure 3C).

Distribution of m⁶A sites in SAP and control groups

We identified 903 m⁶A peaks distributed on 781 circRNAs and it is reported that circRNAs can be generated from any region of the genome[21]. Therefore, we firstly analyzed the genomic distribution of m⁶A and non-m⁶A circRNAs according to their genomic origins to explore their distribution features. As a results, in non-m⁶A circRNAs, 45.33% were sense overlapping, 21.15% exonic, 26.71% intronic, 4.94% intergenic and a few antisense; in m⁶A circRNAs, 42.78% were sense overlapping, 30.32% exonic, 21.27% intronic, 3.42% intergenic and a few antisense (Figure 4A). These results indicated that the majority of m⁶A and non-m⁶A circRNAs were commonly encoded by sense overlapping sequences and the number of circRNAs that generated from protein-coding genes in m⁶A circRNAs was more than those in non-m⁶A circRNAs.

We further analyzed the distribution of circRNAs with DE m⁶A peaks. The length of DE m⁶A circRNAs was mainly enriched in 1–10 000 base pairs (Figure 4B). Although the host genes of m⁶A circRNAs located in all chromosomes, the dysregulated parts mostly located in chromosomes 4, 9 and 11 (Figure 4C). A previous study reported that most circRNAs that derived from protein-coding genes spanned two or three exons [14]. In this study, the majority of circRNAs from protein-coding genes spanned one or two exons (Figure 4D). Similarly, the majority of m⁶A circRNAs and non-m⁶A

Table 1 Top 20 differently expressed N6-methyladenosine peaks compared with control group

	PeakStart	PeakEnd	circRNA	Regulation	Fold-change	P value
chr15	98658229	98658320	chr15:98656602-98658435-	Up	187.2	3.67392E-09
chr11	74929241	74929540	chr11:74928993-74990215+	Up	172.8	3.92116E-09
chr9	108248361	108248660	chr9:108207543-108263690-	Up	120.034482	3.70238E-08
chr2	153763381	153763760	chr2:153756037-153769786+	Up	106.330434	2.09239E-08
chr18	30281961	30282053	chr18:30276981-30282053+	Up	50.9545454	7.61781E-09
chr19	40346381	40346760	chr19:40314443-40373578-	Up	42.4	0.026929988
chr16	94641481	94641740	chr16:94611419-94694141+	Up	37.6772727	7.9549E-08
chr10	60144412	60144720	chr10:60144413-60144723-	Up	24.9	0.014047401
chr11	44652781	44652825	chr11:44651797-44652825+	Up	23.9	0.007108941
chr7	63895821	63896100	chr7:63891679-63938495-	Up	21.1	0.034908475
chr9	107852341	107852720	chr9:107847268-107860459-	Down	302.6	3.63198E-09
chr8	104143561	104143760	chr8:104143031-104143793+	Down	160.728571	1.15908E-08
chr1	150426881	150427260	chr1:150413021-150442180+	Down	52.095238	1.98141E-08
chr1	13312381	13312680	chr1:13298706-13325802-	Down	51.7	6.86061E-05
chr6	119970581	119970800	chr6:119951703-120038640-	Down	47.4	9.37286E-05
chr11	23271132	23271205	chr11:23261835-23271205+	Down	40.6	0.000442849
chr4	108499346	108499398	chr4:108486454-108508433+	Down	27.79	3.27262E-08
chr9	102619691	102619760	chr9:102618811-102619760-	Down	24.25	4.83147E-07
chr11	32296401	32296600	chr11:32283981-32297161+	Down	24.1	4.96449E-07
chr9	69414201	69414580	chr9:69408311-69432615+	Down	22.6	0.00943617

circRNAs were more commonly encoded by a single or two exons (Figure 4E).

Functional analysis of circRNAs with DE m⁶A peaks

To explore the function of m⁶A circRNAs in SAP, GO analysis and KEGG pathway analysis of circRNAs with the DE m⁶A peaks were performed. Figure 5A presented the top 10 GO terms of circRNAs with upregulated m⁶A peaks from the three aspects: BP, CC and MF. For BP, the most enriched and meaningful GO terms were cellular component organization, macromolecule metabolic process and regulation of developmental process. For CC, the top three terms were focal adhesion, cell-substrate junction and anchoring junction. For MF, the main represented GO terms were C2H2 zinc finger domain binding and protein binding. The top 10 pathways from KEGG pathway analysis for circRNAs with upregulated m⁶A peaks were selected and presented in a bubble chart (Figure 5B). Among them, protein digestion and absorption and regulation of autophagy were the major signaling pathways associated with the SAP progression.

The GO terms of circRNAs with downregulated m⁶A peaks are presented in Figure 5C. For BP, protein-containing complex localization, RNA transport and macromolecule metabolic process were the most enriched and meaningful GO terms. For CC, nucleus, dendrite and dendritic tree were the top three terms. For MF, the main represented GO terms were channel regulator activity, RNA, enzyme and protein binding. As for the KEGG pathway analysis of circRNAs with downregulated m⁶A peaks, RNA transport was the main pathway (Figure 5D).

Relationship between m⁶A level and expression of circRNAs in SAP

To explore whether m⁶A modification could affect the expression of circRNAs, we analyzed the expression of m⁶A circRNAs. The expression level of these circRNAs with DE m⁶A peaks did not have significant differences (fold-change < 2 or $P > 0.05$; Supplementary Table 1), indicating that m⁶A modification of circRNAs did not influence the expression of circRNAs. To verify this result further, we analyzed the cumulative distribution of circRNA expression between the control and SAP groups

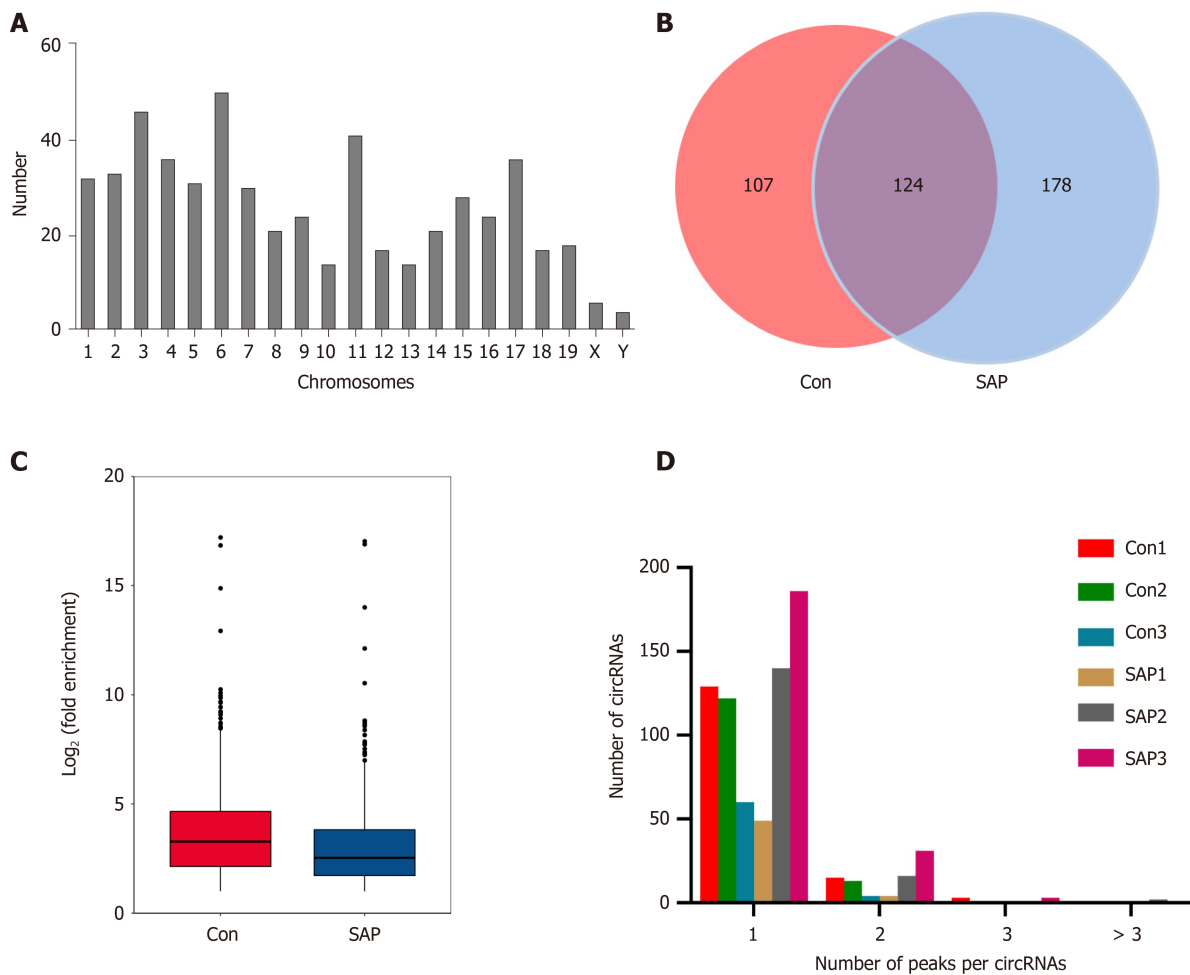


Figure 2 Overview of N⁶-methyladenosine circRNAs in severe acute pancreatitis. A: Number of identified N⁶-methyladenosine (m⁶A) circRNAs according to distribution on chromosomes; B: Venn diagram exhibiting number of common and specific m⁶A circRNAs between control and severe acute pancreatitis (SAP) groups; C: Box plot showing level of m⁶A peaks enrichment in circRNAs in control and SAP groups; D: Number of circRNAs containing variant numbers of m⁶A peaks.

for m⁶A and non-m⁶A circRNAs (Figure 6). This was consistent with the above result.

Construction of m⁶A circRNA–miRNA networks in SAP

Given the importance of circRNA–miRNA interaction[22] and to further explore the underlying mechanism of these circRNAs with DE m⁶A peaks, the top 10 upregulated and top 10 downregulated circRNAs according to the level of m⁶A were selected to construct circRNA–miRNA networks. In this network map, several important miRNAs participated in the occurrence and development of SAP were found to bind to these m⁶A circRNAs (Figure 7), such as miR-24-3p, miR-26a, miR-92b, miR-216b, miR-324-5p and miR-762. These data suggest that these circRNAs with DE m⁶A peaks might play a role in the pathological process of SAP.

Conservation analysis of identified m⁶A circRNAs with human circRNAs

To explore whether the circRNAs with DE m⁶A peaks identified in mouse SAP may have similar roles in human SAP, we performed the conservation analysis of the sequence of the top 10 upregulated and top 10 downregulated circRNAs preliminarily. Through aligning with the sequence of human circRNAs that downloaded from circBase database, we found that 15/20 of the selected circRNAs that have highly similar sequences to human circRNAs (sequence identity > 80%), as shown in the Table 2. These results suggested that these circRNAs may have similar roles in human SAP.

Expression of demethyltransferase in SAP

Given that the total m⁶A level of circRNAs was reduced in SAP and to explore how the m⁶A level was regulated in SAP, we detected the protein and mRNA expression of two

Table 2 The conservation analysis of the sequence between the selected circRNAs and human circRNAs

Mouse circRNA	Human circRNA				
	Human circRNA	Hg19 location	Transcript	Parent gene	Sequence identity, %
chr15:98656602-98658435-	hsa_circ_0026065	chr12:49223538-49245957-	NM_004818	<i>DDX23</i>	88.75
chr11:74928993-74990215+	hsa_circ_0041387	chr17:2139785-2203958-	NM_001170957	<i>SMG6</i>	86.32
chr9:108207543-108263690-	hsa_circ_0124055	chr3:49514281-49548252+	NM_001177634	<i>DAG1</i>	85.36
chr2:153756037-153769786+	hsa_circ_0059811	chr20:31436477-31438211+	NM_012325	<i>MAPRE1</i>	84.18
chr19:40314443-40373578-	hsa_circ_0094611	chr10:97110965-97114724-	ENST00000371247.2	<i>SORBS1</i>	93.52
chr16:94611419-94694141+	hsa_circ_0115989	chr21:38792600-38888974+	ENST00000338785.3	<i>DYRK1A</i>	91.34
chr7:63891679-63938495-	hsa_circ_0034321	chr15:31619082-31670102+	NM_015995	<i>KLF13</i>	85.89
chr9:107847268-107860459-	hsa_circ_0065768	chr3:50000008-50114685+	NM_005777	<i>RBM6</i>	90.84
chr1:150413021-150442180+	hsa_circ_0111511	chr1:186294895-186325581-	NM_003292	<i>TPR</i>	87.91
chr1:13298706-13325802-	hsa_circ_0113369	chr1:42166586-42254891-	ENST00000247584.5	<i>HIVEP3</i>	91.30
chr6:119951703-120038640-	hsa_circ_0024963	chr12:939168-990955+	NM_001184985	<i>WNK1</i>	92.02
chr11:23261835-23271205+	hsa_circ_0120688	chr2:61749745-61764803-	ENST00000404992.2	<i>XPO1</i>	95.11
chr4:108486454-108508433+	hsa_circ_0012539	chr1:52927184-53018762-	NM_001009881	<i>ZCCHC11</i>	92.38
chr11:32283981-32297161+	hsa_circ_0118668	chr2:202780266-202790202-	None	<i>None</i>	91.48
chr9:69408311-69432615+	hsa_circ_0035568	chr15:60720627-60748993-	NM_024611	<i>NARG2</i>	87.08

demethyltransferases (ALKBH5 and FTO). FTO was reduced at the level of protein, but ALKBH5 was increased in SAP at both the level of mRNA and protein (Figure 8). These results indicated that ALKBH5 might be related to the dynamic process of m⁶A in SAP.

DISCUSSION

In the present study, we identified transcriptome-wide map of m⁶A circRNAs and determined their biological significance and potential mechanisms for the first time in SAP. The main findings are: (1) We identified 57 circRNAs with DE m⁶A peaks and found these DE m⁶A circRNAs were involved in the key process of SAP by GO and KEGG analysis, such as protein digestion and regulation of autophagy; (2) In m⁶A circRNA-miRNA networks, several important miRNAs participated in the initiation and development of SAP were found to bind to these m⁶A circRNAs potentially, suggesting that m⁶A may affect the interplays with miRNAs; and (3) The total m⁶A level was reduced in SAP, and the demethylase ALKBH5 was found to be upregulated in SAP, indicating that ALKBH5 may be related to dynamic process of m⁶A in SAP. These results suggested that m⁶A modification on circRNAs may be involved in the pathophysiology of SAP, which may provide novel insights to explore the possible pathophysiological mechanism of SAP and seek new potential therapeutic targets.

To find effective therapeutic targets for SAP, many studies have explored the underlying molecular mechanisms of SAP. Our previous study found that many circRNAs are expressed in mice with SAP[9] and these circRNAs play an important role in the pathogenetic mechanism of SAP[9,23]. In recent years, m⁶A modification of circRNAs was found to be widespread[14] and gained widespread attention in epigenetics. Several important studies have investigated the roles of m⁶A modification in circRNA metabolism and found that m⁶A circRNAs play key roles in some diseases [16,24-28]. In circRNA metabolism, m⁶A modifications can regulate its translation through recognition by YTHDF3 and eIF4G2, and this progress of translation can be enhanced by METTL3/14 and inhibited by FTO[24,25]. In addition, m⁶A circRNAs associate with YTHDF2 in an HRSP12-dependent manner and are selectively downregulated by RNase P/MRP[26]. In innate immunity, Chen *et al*[27] found that unmodified circRNA adjuvant induces antigen-specific T and B cell responses, but m⁶A modification could abrogate circRNA immunity though YTHDF2-mediated suppression. In male germ cells, the back splicing tends to occur mainly at m⁶A-

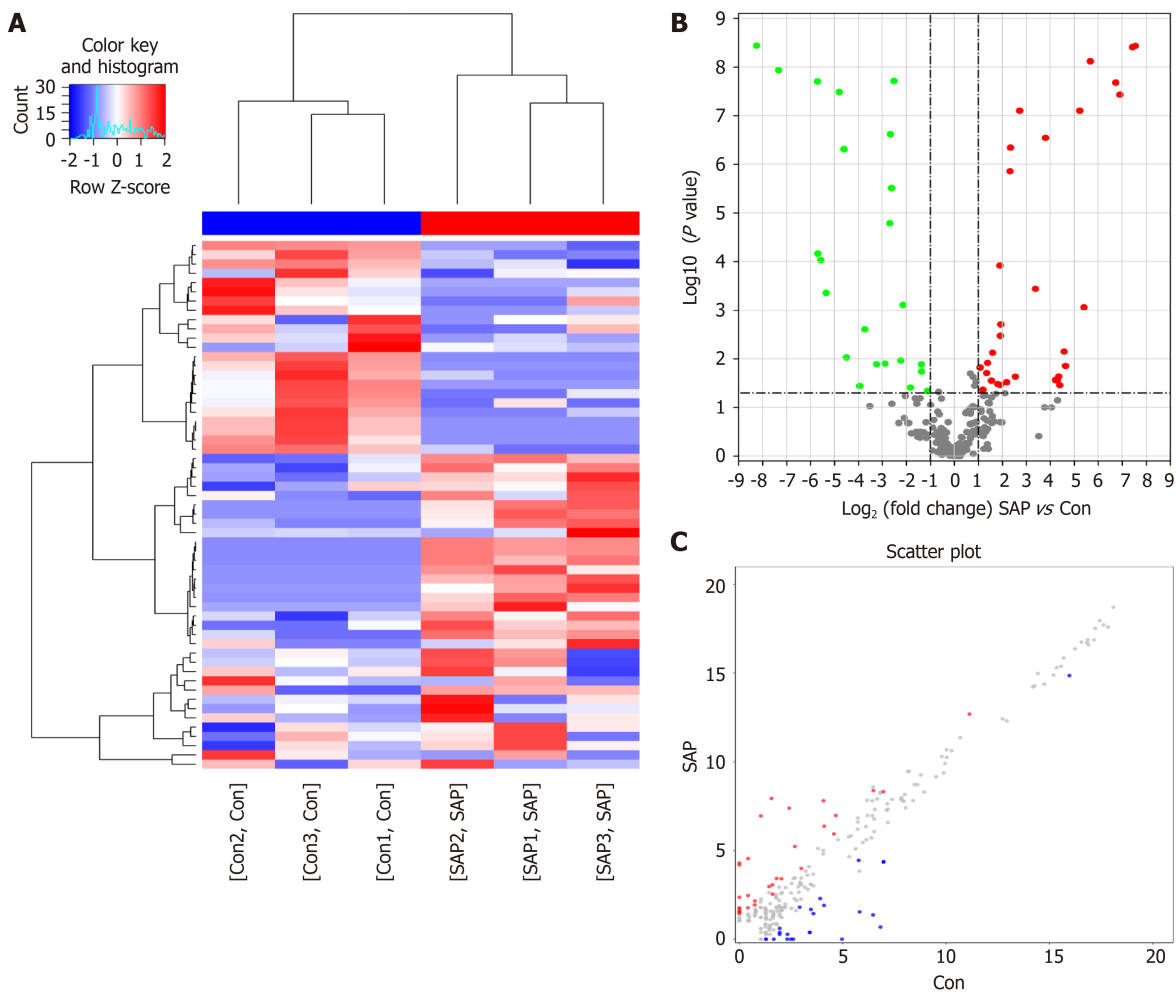


Figure 3 Differential N⁶-methyladenosine modification of circRNAs in severe acute pancreatitis. A: Hierarchical clustering graph exhibiting differential N⁶-methyladenosine (m⁶A) modification of circRNAs in control and severe acute pancreatitis (SAP) groups. Higher expression is presented in red and lower expression in blue; B and C: Volcano and scatter plot showing the circRNAs with significant differentially expressed m⁶A peaks.

enriched sites, which are usually located around the start and stop codons in linear mRNAs, resulting in about half of circRNAs containing large open reading frames. This potential mechanism could ensure long-lasting and stable protein production for specific physiological processes when lacking the corresponding linear mRNAs[28]. These findings showed the important roles of m⁶A in circRNAs during disease progress. Therefore, it is essential to explore the roles of m⁶A circRNAs in SAP.

In the present study, the function analysis of DE m⁶A circRNAs in SAP found that two important pathways were involved in the pathogenesis of SAP, including protein digestion and regulation of autophagy. As an important pathological cellular event, the activation of premature trypsinogen can result in acinar cell necrosis[1]. Many pancreatic injury factors, such as trauma, obstruction of the pancreatic duct and alcohol, can initiate the fusion of lysosomes with zymogen in acinar cells, leading to the activation of trypsinogen through cathepsin B to trypsin. Once trypsin is released, it can cause self-digestion in and outside the acinar cells, and the release of cathepsin B can cause necroptosis. As a cytoprotective mechanism, autophagy can process and recycle various aged, defective or damaged cytoplasmic contents[29]. Selective macroautophagy is a biological process during which specific damaged organelles and misfolded proteins are processed and recycled. Autophagy is accomplished *via* a series of steps, which start with the enucleation of cytoplasmic inclusions in the open double membrane formed by the ER, Golgi apparatus and plasma membrane[30]. Knocking out *ATG7* genes (which are important to form autophagosome) and *LAMP* genes could lead to pancreatitis with extensive inflammation in mice[29,31]. Importantly, impaired autophagy leads to trypsinogen activation, ER stress and mitochondrial dysfunction. These events can together make acinar cells become more susceptible to other insults and cellular death[1]. In addition, RNA transport is enriched in GO terms of note, and Chen *et al*[16] found that m⁶A modification can modulate the export of circNSUN2 to

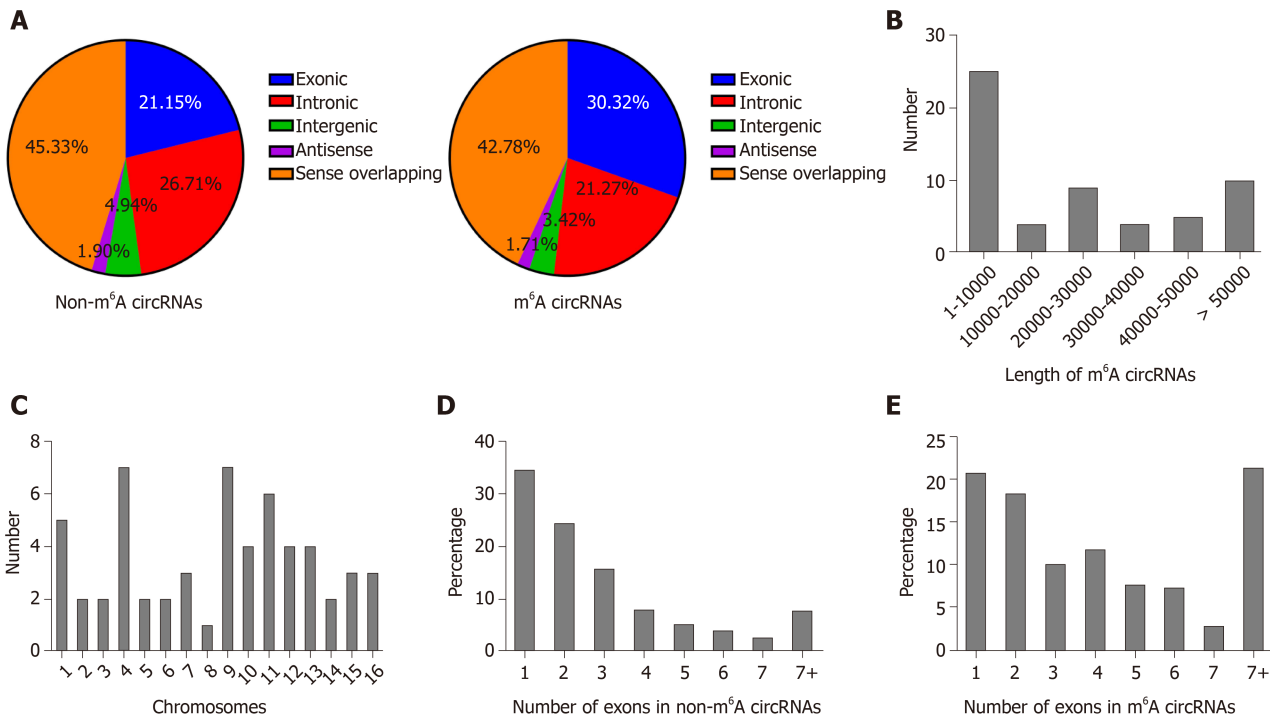


Figure 4 Distribution of N⁶-methyladenosine sites in severe acute pancreatitis and control groups. A: Distribution of genomic origins of non-N⁶-methyladenosine (m⁶A) circRNAs (left) and m⁶A circRNAs (right); B: Number of circRNAs with differentially expressed m⁶A peaks based on the distribution of length; C: Chromosomal distribution of all differential m⁶A sites within circRNAs; D and E: Distribution of non-m⁶A and m⁶A circRNAs based on the number of exons in each circRNA.

the cytoplasm, suggesting that m⁶A modification regulates transport of circRNAs in SAP. These results were consistent with the hypothesis that m⁶A modification of circRNAs participated in the progression of SAP.

m⁶A modification of mRNA can influence its expression by regulating transcription, splicing and degradation[32]. In circRNAs, Zhou *et al*[14] and Su *et al*[33] reported that m⁶A levels are correlated with expression levels of circRNAs in HeLa cells and a rat model of hypoxia-mediated pulmonary hypertension. However, in SAP, we found m⁶A modification in circRNAs was not associated with expression of circRNAs, suggesting that m⁶A circRNAs function in SAP through other mechanisms, such as miRNA sponges. It is worth mentioning that more direct evidence is currently needed to support that m⁶A can affect circRNA expression.

miRNA sponges is an important function of circRNAs. Cytoplasmic circRNAs can prevent miRNAs from binding to target mRNAs by competitive binding to miRNA response elements, further playing a key role in diseases[8,34]. For instance, in lung squamous cell carcinoma, circTP63 can competitively bind to miR-873-3p and prevent miR-873-3p from decreasing the level of FOXM1. The FOXM1 can upregulate the expression of CENPA and CENPB, ultimately facilitating cell cycle progression[35]. In SAP, circHIPK3 can enhance pyroptosis *via* regulating the miR-193a-5p/GSDMD axis in acinar cells, ultimately aggravating this disease[36]. In our previous study, we found that circZFP644 could sponge miR-21-3p, thereby participating in the pathogenesis of SAP[9]. Recently, Su *et al*[33] found that m⁶A modification of circRNAs could influence the interactions between circRNAs and miRNAs. Therefore, analysis of m⁶A circRNA-miRNA networks was performed in this study. Several important miRNAs participated in the pathological process of SAP were found to bind to these m⁶A circRNAs, such as miR-24-3p, miR-26a, miR-92b, miR-216b, miR-324-5p and miR-762. For example, in caerulein-stimulated AR42J cells, expression of miR-92b-3p was decreased, while overexpression of miR-92b-3p could downregulate the expression of TRAF3 and inhibit the MKK3-p38 pathway, attenuating inflammatory response and autophagy[37]. These results suggest that m⁶A modification of circRNAs functions by influencing the interactions between circRNAs and miRNAs.

m⁶A modification is a reversible process that occurs by methyltransferase complex consisting of METTL3, METTL14 and WTAP, and is “erased” by ALKBH5 and FTO [13,15]. In pancreatic cancer, ALKBH5 could regulate the post-transcriptional activation of PER1 through m⁶A abolishment, thereby inhibiting the cancer[38]. In

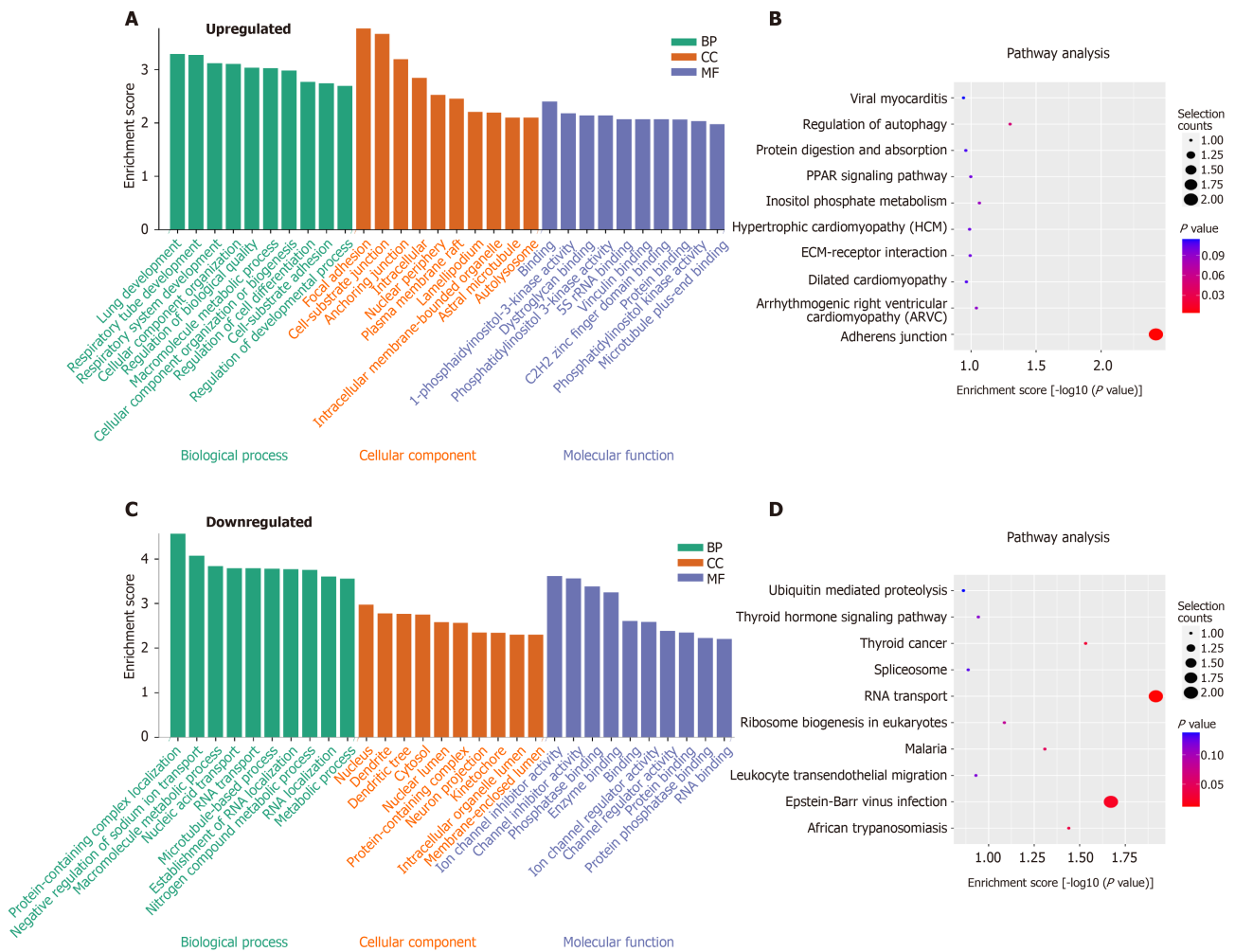


Figure 5 Functional analysis of circRNAs with differentially expressed N⁶-methyladenosine peaks through gene ontology and Kyoto Encyclopedia of Genes and Genomes analysis. A and B: Gene ontology (GO) and Kyoto Encyclopedia of Genes and Genomes (KEGG) analysis of circRNAs with upregulated N⁶-methyladenosine (m⁶A) peaks; C and D: GO and KEGG analysis of circRNAs with downregulated m⁶A peaks. GO analysis include biological process (BP) analysis, cellular component (CC) analysis, and molecular function (MF) analysis.

hepatocellular carcinoma, ALKBH5 could attenuate expression of LYPD1 by an m⁶A-dependent manner and act as a tumor suppressor[39]. Overall, this evidence has suggested that ALKBH5 plays an essential role in m⁶A modification. In this study, we found that expression level of ALKBH5 was upregulated in SAP. Consistent with this result, total m⁶A level of circRNAs in SAP was reduced, indicating that ALKBH5 may play a role in the dynamic process of m⁶A in SAP.

However, there are still limitations in our study. Firstly, further *in vivo* and *in vitro* experiments are needed to further explore the m⁶A circRNA-mediated precise regulatory mechanisms in SAP. Secondly, the conservation analysis of the m⁶A circRNAs showed that these circRNAs may have similar roles in human SAP. However, their clinical significance and the results should be investigated further in SAP patients. Additionally, the precise mechanism of ALKBH5 in m⁶A circRNAs during SAP needs to be studied. Actually, these are in our next plans to explore the roles of m⁶A circRNAs in SAP.

CONCLUSION

In conclusion, our study identified the transcriptome-wide profiling of m⁶A circRNAs in SAP and predicted their biological significance and possible potential mechanisms, providing new insights to explore the possible pathophysiological mechanism of SAP and seek new potential therapeutic targets.

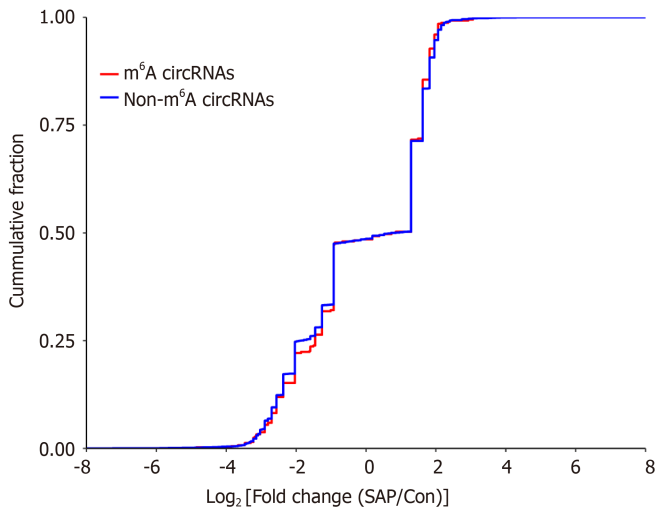


Figure 6 Relationship between N⁶-methyladenosine level and expression of circRNAs in severe acute pancreatitis. Cumulative distribution of circRNAs expression between control and severe acute pancreatitis (SAP) groups for N⁶-methyladenosine (m⁶A) circRNAs (red) and non-m⁶A circRNAs (blue).

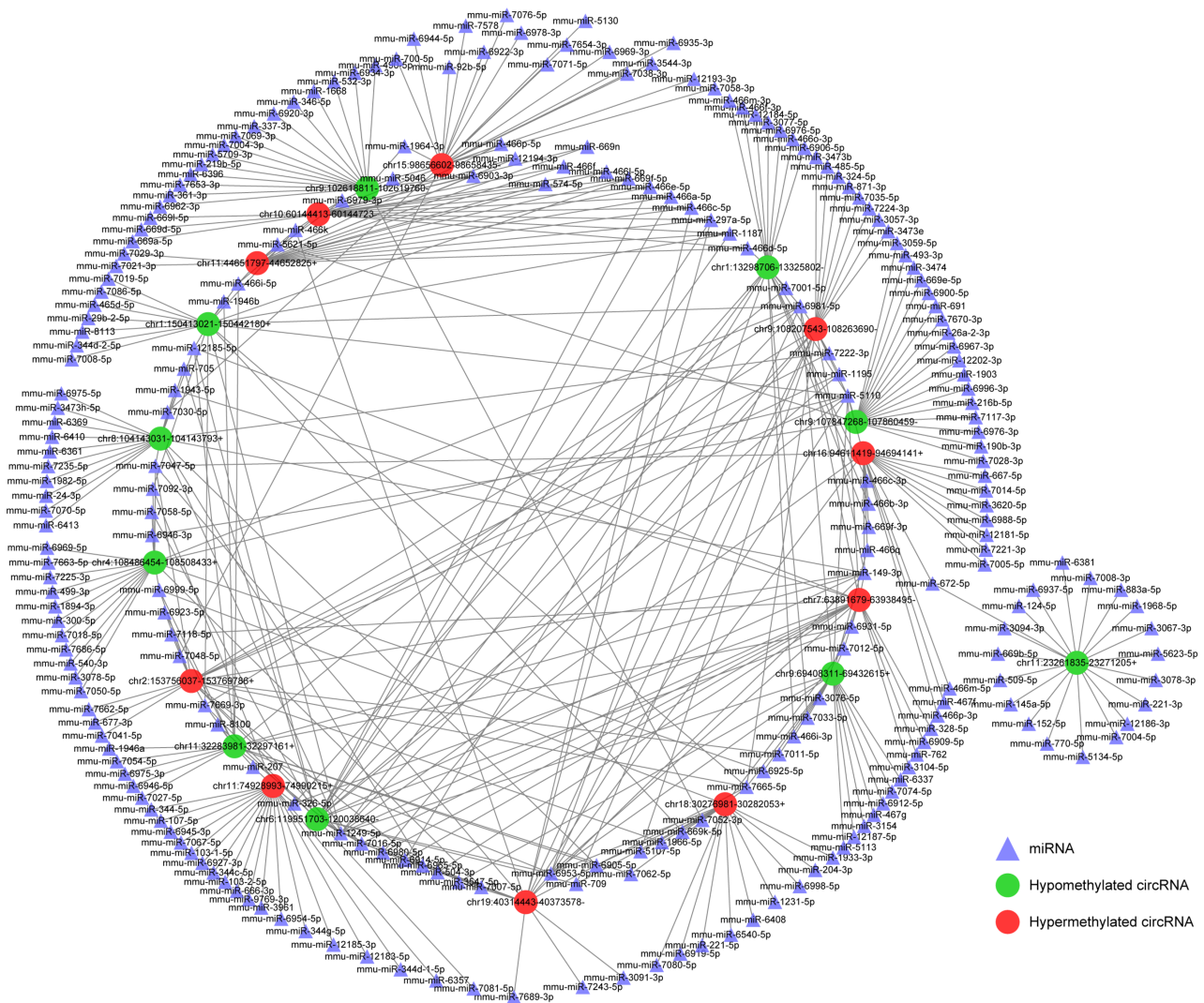


Figure 7 Construction of N⁶-methyladenosine circRNA-miRNA networks in severe acute pancreatitis. A map showing the interaction networks of the top 10 upregulated and top 10 downregulated circRNAs according to the level of N⁶-methyladenosine, and their around 20 target miRNAs with the most stable binding in SAP. Green circles represent hypomethylated circRNAs, red circles represent hypermethylated circRNAs and triangles represent miRNAs, compared with control group.

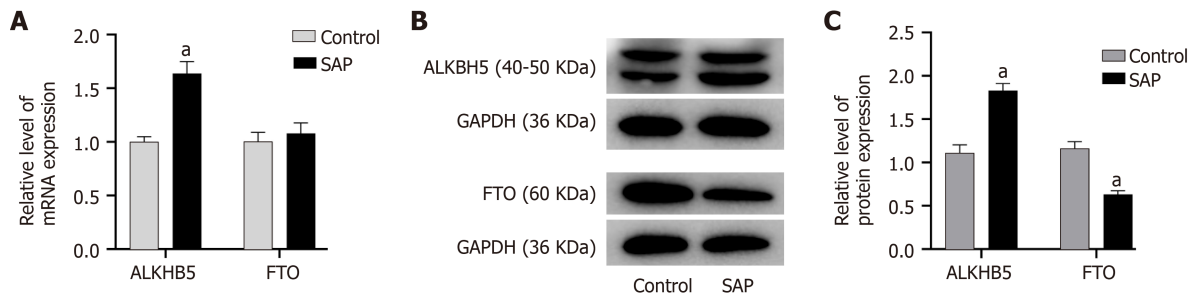


Figure 8 Expression of demethyltransferase in severe acute pancreatitis. A: Relative mRNA levels of alkylation repair homolog 5 (ALKBH5) and fat mass and obesity related protein (FTO) (normalized by the quantity of GAPDH) in each group; B: Representative images of western blot detected with alkylation repair homolog 5 (ALKBH5), FTO, and GAPDH antibodies in control and severe acute pancreatitis (SAP) groups; C: Relative protein levels of ALKBH5 and FTO (measured as the ratio of ALKBH5, FTO to GAPDH by band density) in each group. Data are representative of at least three independent experiments. ^a*P* < 0.05 vs control group.

ARTICLE HIGHLIGHTS

Research background

Severe acute pancreatitis (SAP) is a lethal inflammatory disease with mortality up to 30%. But the genetic pathological mechanism of SAP remains unclear and SAP is still lack of effective therapeutic options. N⁶-methyladenosine (m⁶A) modification of circular (circ)RNAs plays a key role in many diseases and physiological processes through regulating the metabolism and function of circRNAs. However, the role of m⁶A circRNA in SAP has been unexplored yet.

Research motivation

The pathophysiology of SAP at the level of gene regulation is complex and remains unclear. circRNAs are found to participate in many physiological processes and play key roles in pathological processes during SAP. m⁶A modification can affect the “fate” of m⁶A modified circRNAs, thereby participating in the regulation of diseases. Therefore, we want to explore whether the m⁶A modification of circRNAs is related to the pathophysiological mechanism of SAP, and determine their biological significance and potential mechanisms.

Research objectives

The present study aims to determine the transcriptome-wide map of m⁶A circRNAs and explore their biological significance and its possible mechanisms in SAP.

Research methods

The SAP C57BL/6 mice model was induced by retrograde injection of 4% sodium taurocholate salt. m⁶A-modified RNA immunoprecipitation sequencing was used to determine the transcriptome-wide map of m⁶A circRNAs. The biological significance of circRNAs with differentially expressed m⁶A peaks was identified by GO and KEGG analysis. m⁶A circRNA-microRNA networks was constructed to explore the underlying mechanism of m⁶A circRNAs in SAP. The expression of demethylases was measured by western blot and qPCR. H&E staining and measurement of serum lipase and amylase were performed to assess the establishment of SAP mice model.

Research results

In the identified transcriptome-wide map of m⁶A circRNAs, there were 57 circRNAs with differentially expressed m⁶A peaks; among which, 32 were upregulated and 25 downregulated. Important pathways in the pathogenetic process during SAP were found by functional analysis of these m⁶A circRNAs, such as protein digestion and regulation of autophagy. m⁶A circRNA-miRNA networks showed that several important miRNAs in pathogenesis of SAP were bind to these m⁶A circRNAs, such as miR-24-3p, miR-26a, miR-92b, miR-216b, miR-324-5p and miR-762. To be note, the total m⁶A level of circRNAs was reduced in SAP, accompanied by the upregulated demethylase ALKBH5.

Research conclusions

The transcriptome-wide profiling of m⁶A circRNAs in SAP was identified, and the

biological significance and possible potential mechanisms of m⁶A circRNAs in SAP were predicted, providing new insights into exploring the possible pathophysiological mechanism of SAP and new potential therapeutic targets.

Research perspectives

This present study for the first time identified transcriptome-wide map of m⁶A circRNAs and determined their biological significance and potential mechanisms. However, the m⁶A circRNA-mediated precise regulatory mechanisms are need to be explore further *in vivo* and *in vitro* experiments. What's more, further studies are needed to reveal the precise mechanism of ALKBH5 in m⁶A circRNAs during SAP. In the future, we will explore them and investigate these m⁶A circRNAs in SAP patients.

REFERENCES

- Lee PJ, Papachristou GI. New insights into acute pancreatitis. *Nat Rev Gastroenterol Hepatol* 2019; **16**: 479-496 [PMID: 31138897 DOI: 10.1038/s41575-019-0158-2]
- Trikudanathan G, Wolbrink DRJ, van Santvoort HC, Mallory S, Freeman M, Besselink MG. Current Concepts in Severe Acute and Necrotizing Pancreatitis: An Evidence-Based Approach. *Gastroenterology* 2019; **156**: 1994-2007.e3 [PMID: 30776347 DOI: 10.1053/j.gastro.2019.01.269]
- Garg PK, Singh VP. Organ Failure Due to Systemic Injury in Acute Pancreatitis. *Gastroenterology* 2019; **156**: 2008-2023 [PMID: 30768987 DOI: 10.1053/j.gastro.2018.12.041]
- Hsu MT, Coca-Prados M. Electron microscopic evidence for the circular form of RNA in the cytoplasm of eukaryotic cells. *Nature* 1979; **280**: 339-340 [PMID: 460409 DOI: 10.1038/280339a0]
- Meng X, Li X, Zhang P, Wang J, Zhou Y, Chen M. Circular RNA: an emerging key player in RNA world. *Brief Bioinform* 2017; **18**: 547-557 [PMID: 27255916 DOI: 10.1093/bib/bbw045]
- Panda AC, Grammatikakis I, Munk R, Gorospe M, Abdelmohsen K. Emerging roles and context of circular RNAs. *Wiley Interdiscip Rev RNA* 2017; **8** [PMID: 27612318 DOI: 10.1002/wrna.1386]
- Barrett SP, Salzman J. Circular RNAs: analysis, expression and potential functions. *Development* 2016; **143**: 1838-1847 [PMID: 27246710 DOI: 10.1242/dev.128074]
- Aufiero S, Reckman YJ, Pinto YM, Creemers EE. Circular RNAs open a new chapter in cardiovascular biology. *Nat Rev Cardiol* 2019; **16**: 503-514 [PMID: 30952956 DOI: 10.1038/s41569-019-0185-2]
- Yang Y, Ren J, Huang Q, Wu J, Yuan X, Jiang W, Wen Y, Tang L, Sun H. CircRNA Expression Profiles and the Potential Role of CircZFP644 in Mice With Severe Acute Pancreatitis via Sponging miR-21-3p. *Front Genet* 2020; **11**: 206 [PMID: 32226441 DOI: 10.3389/fgene.2020.00206]
- Meng S, Zhou H, Feng Z, Xu Z, Tang Y, Li P, Wu M. CircRNA: functions and properties of a novel potential biomarker for cancer. *Mol Cancer* 2017; **16**: 94 [PMID: 28535767 DOI: 10.1186/s12943-017-0663-2]
- Dube U, Del-Aguila JL, Li Z, Budde JP, Jiang S, Hsu S, Ibanez L, Fernandez MV, Farias F, Norton J, Gentsch J, Wang F; Dominantly Inherited Alzheimer Network (DIAN), Salloway S, Masters CL, Lee JH, Graff-Radford NR, Chhatwal JP, Bateman RJ, Morris JC, Karch CM, Harari O, Cruchaga C. An atlas of cortical RNA expression in Alzheimer disease brains demonstrates clinical and pathological associations. *Nat Neurosci* 2019; **22**: 1903-1912 [PMID: 31591557 DOI: 10.1038/s41593-019-0501-5]
- Chen X, Yang T, Wang W, Xi W, Zhang T, Li Q, Yang A, Wang T. Circular RNAs in immune responses and immune diseases. *Theranostics* 2019; **9**: 588-607 [PMID: 30809295 DOI: 10.7150/thno.29678]
- Shulman Z, Stern-Ginossar N. The RNA modification N⁶-methyladenosine as a novel regulator of the immune system. *Nat Immunol* 2020; **21**: 501-512 [PMID: 32284591 DOI: 10.1038/s41590-020-0650-4]
- Zhou C, Molinie B, Daneshvar K, Pondick JV, Wang J, Van Wittenberghe N, Xing Y, Giallourakis CC, Mullen AC. Genome-Wide Maps of m⁶A circRNAs Identify Widespread and Cell-Type-Specific Methylation Patterns that Are Distinct from mRNAs. *Cell Rep* 2017; **20**: 2262-2276 [PMID: 28854373 DOI: 10.1016/j.celrep.2017.08.027]
- Zhang L, Hou C, Chen C, Guo Y, Yuan W, Yin D, Liu J, Sun Z. The role of N⁶-methyladenosine (m⁶A) modification in the regulation of circRNAs. *Mol Cancer* 2020; **19**: 105 [PMID: 32522202 DOI: 10.1186/s12943-020-01224-3]
- Chen RX, Chen X, Xia LP, Zhang JX, Pan ZZ, Ma XD, Han K, Chen JW, Judde JG, Deas O, Wang F, Ma NF, Guan X, Yun JP, Wang FW, Xu RH, Dan Xie. N⁶-methyladenosine modification of circNSUN2 facilitates cytoplasmic export and stabilizes HMGA2 to promote colorectal liver metastasis. *Nat Commun* 2019; **10**: 4695 [PMID: 31619685 DOI: 10.1038/s41467-019-12651-2]
- Schmidt J, Rattner DW, Lewandrowski K, Compton CC, Mandavilli U, Knoefel WT, Warshaw AL. A better model of acute pancreatitis for evaluating therapy. *Ann Surg* 1992; **215**: 44-56 [PMID: 1731649 DOI: 10.1097/0000658-199201000-00007]
- Ashburner M, Ball CA, Blake JA, Botstein D, Butler H, Cherry JM, Davis AP, Dolinski K, Dwight SS, Eppig JT, Harris MA, Hill DP, Issel-Tarver L, Kasarskis A, Lewis S, Matese JC, Richardson JE, Ringwald M, Rubin GM, Sherlock G. Gene ontology: tool for the unification of biology. *The Gene*

- Ontology Consortium. *Nat Genet* 2000; **25**: 25-29 [PMID: 10802651 DOI: 10.1038/75556]
- 19 Thomson DW, Dinger ME. Endogenous microRNA sponges: evidence and controversy. *Nat Rev Genet* 2016; **17**: 272-283 [PMID: 27040487 DOI: 10.1038/nrg.2016.20]
 - 20 Crockett SD, Wani S, Gardner TB, Falck-Ytter Y, Barkun AN; American Gastroenterological Association Institute Clinical Guidelines Committee. American Gastroenterological Association Institute Guideline on Initial Management of Acute Pancreatitis. *Gastroenterology* 2018; **154**: 1096-1101 [PMID: 29409760 DOI: 10.1053/j.gastro.2018.01.032]
 - 21 Qu S, Zhong Y, Shang R, Zhang X, Song W, Kjems J, Li H. The emerging landscape of circular RNA in life processes. *RNA Biol* 2017; **14**: 992-999 [PMID: 27617908 DOI: 10.1080/15476286.2016.1220473]
 - 22 Panda AC. Circular RNAs Act as miRNA Sponges. *Adv Exp Med Biol* 2018; **1087**: 67-79 [PMID: 30259358 DOI: 10.1007/978-981-13-1426-1_6]
 - 23 Wang B, Wu J, Huang Q, Yuan X, Yang Y, Jiang W, Wen Y, Tang L, Sun H. Comprehensive Analysis of Differentially Expressed lncRNA, circRNA and mRNA and Their ceRNA Networks in Mice With Severe Acute Pancreatitis. *Front Genet* 2021; **12**: 625846 [PMID: 33584827 DOI: 10.3389/fgene.2021.625846]
 - 24 Di Timoteo G, Dattilo D, Centrón-Broco A, Colantoni A, Guarnacci M, Rossi F, Incarnato D, Oliviero S, Fatica A, Morlando M, Bozzoni I. Modulation of circRNA Metabolism by m⁶A Modification. *Cell Rep* 2020; **31**: 107641 [PMID: 32402287 DOI: 10.1016/j.celrep.2020.107641]
 - 25 Yang Y, Fan X, Mao M, Song X, Wu P, Zhang Y, Jin Y, Yang Y, Chen LL, Wang Y, Wong CC, Xiao X, Wang Z. Extensive translation of circular RNAs driven by N⁶-methyladenosine. *Cell Res* 2017; **27**: 626-641 [PMID: 28281539 DOI: 10.1038/cr.2017.31]
 - 26 Park OH, Ha H, Lee Y, Boo SH, Kwon DH, Song HK, Kim YK. Endoribonucleolytic Cleavage of m⁶A-Containing RNAs by RNase P/MRP Complex. *Mol Cell* 2019; **74**: 494-507.e8 [PMID: 30930054 DOI: 10.1016/j.molcel.2019.02.034]
 - 27 Chen YG, Chen R, Ahmad S, Verma R, Kasturi SP, Amaya L, Broughton JP, Kim J, Cadena C, Pulendran B, Hur S, Chang HY. N6-Methyladenosine Modification Controls Circular RNA Immunity. *Mol Cell* 2019; **76**: 96-109.e9 [PMID: 31474572 DOI: 10.1016/j.molcel.2019.07.016]
 - 28 Tang C, Xie Y, Yu T, Liu N, Wang Z, Woolsey RJ, Tang Y, Zhang X, Qin W, Zhang Y, Song G, Zheng W, Wang J, Chen W, Wei X, Xie Z, Klukovich R, Zheng H, Quilici DR, Yan W. m⁶A-dependent biogenesis of circular RNAs in male germ cells. *Cell Res* 2020; **30**: 211-228 [PMID: 32047269 DOI: 10.1038/s41422-020-0279-8]
 - 29 Antonucci L, Fagman JB, Kim JY, Todoric J, Gukovsky I, Mackey M, Ellisman MH, Karin M. Basal autophagy maintains pancreatic acinar cell homeostasis and protein synthesis and prevents ER stress. *Proc Natl Acad Sci U S A* 2015; **112**: E6166-E6174 [PMID: 26512112 DOI: 10.1073/pnas.1519384112]
 - 30 Gukovskaya AS, Gukovsky I, Algül H, Habtezion A. Autophagy, Inflammation, and Immune Dysfunction in the Pathogenesis of Pancreatitis. *Gastroenterology* 2017; **153**: 1212-1226 [PMID: 28918190 DOI: 10.1053/j.gastro.2017.08.071]
 - 31 Mareninova OA, Hermann K, French SW, O'Konski MS, Pandol SJ, Webster P, Erickson AH, Katunuma N, Gorelick FS, Gukovsky I, Gukovskaya AS. Impaired autophagic flux mediates acinar cell vacuole formation and trypsinogen activation in rodent models of acute pancreatitis. *J Clin Invest* 2009; **119**: 3340-3355 [PMID: 19805911 DOI: 10.1172/JCI38674]
 - 32 Zhu ZM, Huo FC, Pei DS. Function and evolution of RNA N6-methyladenosine modification. *Int J Biol Sci* 2020; **16**: 1929-1940 [PMID: 32398960 DOI: 10.7150/ijbs.45231]
 - 33 Su H, Wang G, Wu L, Ma X, Ying K, Zhang R. Transcriptome-wide map of m⁶A circRNAs identified in a rat model of hypoxia mediated pulmonary hypertension. *BMC Genomics* 2020; **21**: 39 [PMID: 31931709 DOI: 10.1186/s12864-020-6462-y]
 - 34 Salmena L, Poliseno L, Tay Y, Kats L, Pandolfi PP. A ceRNA hypothesis: the Rosetta Stone of a hidden RNA language? *Cell* 2011; **146**: 353-358 [PMID: 21802130 DOI: 10.1016/j.cell.2011.07.014]
 - 35 Cheng Z, Yu C, Cui S, Wang H, Jin H, Wang C, Li B, Qin M, Yang C, He J, Zuo Q, Wang S, Liu J, Ye W, Lv Y, Zhao F, Yao M, Jiang L, Qin W. circTP63 functions as a ceRNA to promote lung squamous cell carcinoma progression by upregulating FOXM1. *Nat Commun* 2019; **10**: 3200 [PMID: 31324812 DOI: 10.1038/s41467-019-11162-4]
 - 36 Wang J, Li X, Liu Y, Peng C, Zhu H, Tu G, Yu X, Li Z. CircHIPK3 Promotes Pyroptosis in Acinar Cells Through Regulation of the miR-193a-5p/GSDMD Axis. *Front Med (Lausanne)* 2020; **7**: 88 [PMID: 32318575 DOI: 10.3389/fmed.2020.00088]
 - 37 Sun H, Tian J, Li J. MiR-92b-3p ameliorates inflammation and autophagy by targeting TRAF3 and suppressing MKK3-p38 pathway in caerulein-induced AR42J cells. *Int Immunopharmacol* 2020; **88**: 106691 [PMID: 32822908 DOI: 10.1016/j.intimp.2020.106691]
 - 38 Guo X, Li K, Jiang W, Hu Y, Xiao W, Huang Y, Feng Y, Pan Q, Wan R. RNA demethylase ALKBH5 prevents pancreatic cancer progression by posttranscriptional activation of PER1 in an m⁶A-YTHDF2-dependent manner. *Mol Cancer* 2020; **19**: 91 [PMID: 32429928 DOI: 10.1186/s12943-020-01158-w]
 - 39 Chen Y, Zhao Y, Chen J, Peng C, Zhang Y, Tong R, Cheng Q, Yang B, Feng X, Lu Y, Xie H, Zhou L, Wu J, Zheng S. ALKBH5 suppresses malignancy of hepatocellular carcinoma via m⁶A-guided epigenetic inhibition of LYPD1. *Mol Cancer* 2020; **19**: 123 [PMID: 32772918 DOI: 10.1186/s12943-020-01239-w]



Published by **Baishideng Publishing Group Inc**
7041 Koll Center Parkway, Suite 160, Pleasanton, CA 94566, USA
Telephone: +1-925-3991568
E-mail: bpgoffice@wjgnet.com
Help Desk: <https://www.f6publishing.com/helpdesk>
<https://www.wjgnet.com>

